Monthly Notices
of the
ROYAL ASTRONOMICAL SOCIETY

Mon. Not. R. Astron. Soc. **418,** 2336–2342 (2011) doi:10.1111/j.1365-2966.2011.19623.x

Optimum frequency band for radio polarization observations

Tigran G. Arshakian[1,2]★ and Rainer Beck[1]

[1]*Max-Planck-Institut für Radioastronomie, Auf dem Hügel 69, 53121 Bonn, Germany*
[2]*Byurakan Astrophysical Observatory, Aragatsotn prov. 378433, Armenia and Isaac Newton Institute of Chile, Armenian Branch*

Accepted 2011 August 11. Received 2011 July 24; in original form 2011 April 20

ABSTRACT

Polarized radio synchrotron emission from interstellar, intracluster and intergalactic magnetic fields is affected by frequency-dependent Faraday depolarization. The maximum polarized intensity depends on the physical properties of the depolarizing medium. New-generation radio telescopes such as Low Frequency Array (LOFAR), the Square Kilometre Array (SKA) and its precursors need a wide range of frequencies to cover the full range of objects. The optimum frequency of maximum polarized intensity (PI) is computed for the cases of depolarization in magneto-ionic media by regular magnetic fields (differential Faraday rotation) or by turbulent magnetic fields (internal or external Faraday dispersion), assuming that the Faraday spectrum of the medium is dominated by one component or that the medium is turbulent. Polarized emission from bright galaxy discs, spiral arms and cores of galaxy clusters are best observed at wavelengths below a few centimetres (at frequencies beyond about 10 GHz), haloes of galaxies and clusters around decimetre wavelengths (at frequencies below about 2 GHz). Intergalactic filaments need observations at metre wavelengths (frequencies below 300 MHz). Sources with extremely large intrinsic rotation measure |RM| or RM dispersion can be searched with mm-wave telescopes. Measurement of the PI spectrum allows us to derive the average Faraday |RM| or the Faraday dispersion within the source, as demonstrated for the case of the spiral galaxy NGC 6946. Periodic fluctuations in PI at low frequencies are a signature of differential Faraday rotation. Internal and external Faraday dispersion can be distinguished by the different slopes of the PI spectrum at low frequencies. A wide band around the optimum frequency is important to distinguish between varieties of depolarization effects.

Key words: techniques: polarimetric – ISM: magnetic fields – galaxies: clusters: general – galaxies: haloes – galaxies: magnetic fields – radio continuum: galaxies.

1 INTRODUCTION

The major radio continuum surveys planned with future radio facilities such as the Square Kilometre Array (SKA), its precursor telescopes Australian Square Kilometre Array Pathfinder (ASKAP), Karoo Array Telescope (MeerKAT) and Aprerture Tile in Focus (APERTIF), and low-frequency radio telescopes such as Low Frequency Array (LOFAR) and Murchison Widefield Array (MWA) will open a new era in the study of cosmic magnetic fields via polarized synchrotron emission and Faraday rotation. As these telescopes will operate at different frequencies, it is crucial to investigate which astrophysical objects can be observed with a certain telescope and to select the frequency band that will yield maximum polarized intensity for these objects.

In total radio continuum intensity, many astrophysical sources reveal a power-law synchrotron spectrum with an almost constant spectral index over the radio frequency range where the energy losses of the cosmic ray electrons are small. The total intensity of synchrotron emission depends on the number density of cosmic ray electrons and the strength of the total magnetic field component normal to the line of sight of the observer, while the polarized intensity is related to ordered magnetic fields. Ordered fields can be regular (coherent), generated by the mean-field dynamo (Beck et al. 1996) or anisotropic, generated from turbulent magnetic fields by compressing or shearing gas flows. Turbulent fields with random orientations give rise to unpolarized synchrotron emission. The degree of synchrotron polarization is a function of the ratio between ordered and turbulent fields (Sokoloff et al. 1998).

If the magnetic field structure is not resolved, the degree of polarization is reduced by an effect called *beam depolarization* which depends on the beamsize of the telescope. For the same resolution, the intensity of polarized radio continuum emission is the result of competition between two processes: synchrotron emission and *Faraday depolarization* (DP), both of which increase with wavelength.

★E-mail: tigar@mpifr-bonn.mpg.de

DP is caused by variations in Faraday rotation. Faraday rotation changes the polarization plane when the radio wave passes through a magneto-ionic medium with regular magnetic fields. Hence, Faraday rotation is an important signature of magneto-ionic media containing regular magnetic fields and is a measure of field strength and thermal electron density.

Faraday rotation $\Delta\chi$ is traditionally measured from the polarization angles χ at several wavelengths and quantified by the rotation measure (RM), defined as $\Delta\chi = \mathrm{RM}\Delta\lambda^2$. The $\pm n\pi$ ambiguity of the polarization angle χ requires the determination of RM by the slope of the best fit of the relation between χ and λ^2 – if this relation is linear.

Faraday rotation in a foreground screen in front of the synchrotron-emitting region can be described by a single RM value, which means that the slope of the relation between χ and λ^2 is constant over the whole wavelength range. If, however, Faraday rotation occurs within the emitting region, the observable RM is no longer constant beyond a critical wavelength (Burn 1966): the medium becomes 'Faraday-thick'. Below this critical wavelength, a 'simple' layer can still be characterized by a single value of RM, if the distributions of regular magnetic fields and thermal electrons are box-like ('Burn's slab') or symmetric Gaussians or symmetric exponentials (Sokoloff et al. 1998).

In complex media with several distinct synchrotron-emitting and Faraday-rotating regions within the measured volume, no single RM value exists and *RM synthesis* needs to be applied. It Fourier-transforms the complex polarization (amplitude and angle) measured over a large frequency spread into the complex Faraday spectrum in Faraday depth space (Burn 1966; Brentjens & de Bruyn 2005; Heald 2009; Frick et al. 2010). Modern radio telescopes have a sufficiently large number of frequency channels and large total bandwidth to perform RM synthesis with high resolution in Faraday space.

Present-day data from the Westerbork Synthesis Radio Telescope (WSRT) towards bright regions in the Milky Way and towards galaxy clusters indicate that a significant (possibly dominant) fraction of Faraday spectra show one component or one dominant component (Schnitzeler, Katgert & de Bruyn 2009; Brentjens 2011; Pizzo et al. 2011). Media with turbulent magnetic fields and/or turbulent distribution of thermal electrons are expected to show a turbulent Faraday spectrum (Frick et al. 2011).

If the region contains cosmic ray electrons, thermal electrons and regular magnetic fields, the polarization planes from waves from the far side of the emitting layer are more Faraday-rotated than those from the near side. This leads to wavelength-dependent depolarization, called *differential Faraday rotation* (DFR). Turbulent fields also cause wavelength-dependent depolarization, called *Faraday dispersion*. Internal Faraday dispersion (IFD) occurs in an emitting and Faraday-rotating region, while external Faraday dispersion (EFD) may occur in a non-emitting foreground screen (Burn 1966; Sokoloff et al. 1998). DFR is a function of RM and wavelength (equation 4), while Faraday dispersion depends on RM dispersion and wavelength (equations 8 and 9).

Depolarization of the emission from various cosmic objects varies strongly and depends on coherence length, strength of the regular and turbulent magnetic fields and thermal electron density. Hence, each population of polarized objects should be studied at the optimum wavelength at which the PI is maximum.

The observed spectrum of PI is a power law over a limited wavelength range and often reveals a maximum at a certain wavelength $\lambda_{\max}$ (Kronberg, Conway & Gilbert 1972; Conway et al. 1974; Tabara & Inoue 1980). Below $\lambda_{\max}$, the degree of polarization decreases with decreasing wavelength, called *polarization inversion*. In the case of compact radio sources, polarization inversion is often related to flat-spectrum (opaque) sources and is probably caused by Faraday dispersion (Conway et al. 1974).

In this paper, we investigate the optimum frequency band for polarization observations of various classes of astrophysical objects. We assume that the Faraday spectrum is dominated by one component or that the medium is turbulent. We also explore possibilities of distinguishing between internal/external Faraday dispersion and differential Faraday rotation, which allows investigation of the physical properties of the depolarizing medium in various cosmic objects.

2 OPTIMUM WAVELENGTH FOR MAXIMUM POLARIZED INTENSITY

The total intensity of the synchrotron emission detected in the rest frame of the observer at a frequency ν is

$$I_\nu = C_1 n_{\mathrm{CR}} B_{\mathrm{t},\perp}^{2(1+\alpha)}\, \nu^{-\alpha}\, L, \tag{1}$$

where n_{CR} is the density of cosmic ray electrons (per energy interval) which have a power-law energy spectrum [$N(E) \propto E^{-\gamma}$] with the spectral index γ, leading to the synchrotron spectral index $\alpha = (\gamma - 1)/2$; L is the linear size of the emitting region, and $B_{\mathrm{t},\perp}$ is the strength of the total magnetic field perpendicular to the line of sight.

The PI is given by

$$P_\nu = p_0\, I_\nu \left(\frac{B_{\mathrm{ord},\perp}}{B_{\mathrm{t},\perp}}\right)^2 \mathrm{DP}_\nu, \tag{2}$$

where $p_0 = (1+\gamma)/(7/3+\gamma)$ is the maximum degree of polarization ($p_0 \simeq 0.74$ for a typical spectral index of $\gamma \simeq 2.7$ in galaxies), $B_{\mathrm{ord},\perp}$ is the strength of the ordered (regular + anisotropic[1]) magnetic field perpendicular to the line of sight and DP_ν is the depolarization coefficient. Assuming that the cosmic ray density, total and ordered magnetic fields are stationary, we write

$$P_\nu = C \nu^{-\alpha}\, \mathrm{DP}_\nu, \tag{3}$$

where $C = C_1 p_0 n_{\mathrm{CR}} B_{\mathrm{ord},\perp}^2\, B_{\mathrm{t},\perp}^{\alpha-1}$.

2.1 Differential Faraday rotation

Wavelength-dependent Faraday depolarization occurs in a region containing cosmic ray electrons, thermal electrons and regular magnetic fields. The polarization planes of the waves from different synchrotron-emitting layers are rotated differently: the polarization planes from the near emitting layers rotate less than those emitted from the far layers. This effect is known as DFR and is given by

$$\mathrm{DP} = \frac{|\sin(2\,\mathrm{RM}\,\lambda^2)|}{|2\,\mathrm{RM}\,\lambda^2|}. \tag{4}$$

RM is the average observed rotation measure (in rad m^{-2}),

$$\begin{aligned}\mathrm{RM\,(rad\,m^{-2})} &= 0.81 \int n_{\mathrm{e}} B_{\mathrm{reg},\parallel}\, \mathrm{d}L \\ &\simeq 0.81 \langle n_{\mathrm{e}}\rangle \langle B_{\mathrm{reg},\parallel}\rangle L,\end{aligned} \tag{5}$$

where n_{e} (in cm^{-3}) is the thermal electron density, $B_{\mathrm{reg},\parallel}$ (in μG) is the strength of the regular magnetic field along the line of sight,

[1] An anisotropic field can be generated by compressing or shearing an isotropic turbulent field; it contributes to polarized emission but not to Faraday rotation.

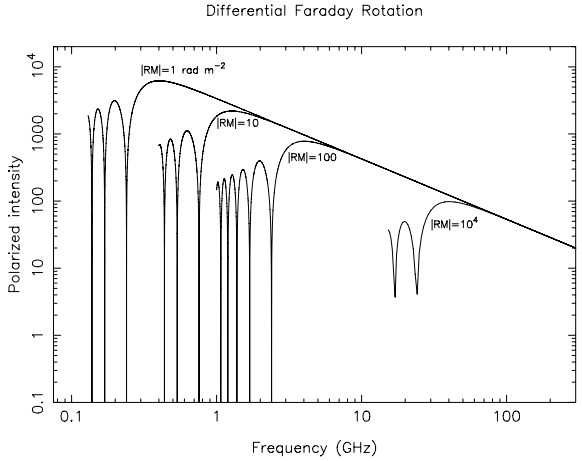

Figure 1. Polarized intensity for a spectral index of total synchrotron intensity of $\alpha = 0.9$ and depolarization by differential Faraday rotation at the level of |RM| = 1, 10, 100 and 10^4 rad m^{-2}.

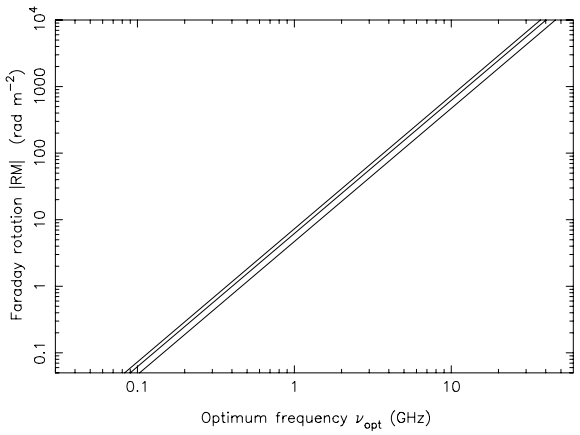

Figure 2. Optimum frequency of maximum polarized emission for a synchrotron spectrum with spectral index $\alpha = 0.5$, 0.9 and 1.3 (from bottom to top) and depolarization by differential Faraday rotation as a function of |RM|.

and L is the path-length through the regular field and thermal gas in parsec (pc). We assume here that the magneto-ionic medium can be characterized by one single RM value, i.e. the distributions of n_e and $B_{reg,\parallel}$ are smooth and symmetric along the line of sight (Sokoloff et al. 1998).

The maximum PI is reached at larger frequencies for larger values of RM (Fig. 1). At low frequencies (before the maximum) the slope of the curve, measured between 1/10 and 1/100 of the maximum PI, is $\alpha \simeq 100$ (Fig. 1). The periodic changes of DP with wavelength (equation 4) lead to total depolarization at certain wavelengths, observable as 'depolarization canals' in maps of polarized emission (e.g. Fletcher & Shukurov 2006). However, 'canals' can also originate from steep gradients in the polarization angle caused e.g. by turbulent fields (Sun et al. 2011).

Accounting for the differential Faraday depolarization (equation 4) and solving the equation $dP_\nu/d\lambda = 0$, we derive a transcendental equation for the optimum wavelength (λ_{opt}) of the maximum polarized emission,

$$|\sin k| - \frac{2k}{2-\alpha}|\cos k| = 0, \tag{6}$$

where $k = 2\,|\mathrm{RM}|\,\lambda_{opt}^2$. We derive the equation

$$\lambda_{opt} = A(\alpha)\,|\mathrm{RM}|^{-0.5}, \tag{7}$$

where λ_{opt} is measured in m and $A(\alpha)$ is 0.65, 0.75 and 0.81 for $\alpha =$ 0.5, 0.9 and 1.3, respectively. The dependence of the optimum frequency (ν_{opt}) on rotation measure for $\alpha = 0.5$, 0.9 and 1.3 is shown in Fig. 2: polarized sources with larger |RM| are best observed at high frequencies.

Note that regions with thermal electrons and a constant regular field, but without cosmic ray electrons (no synchrotron emission), called 'Faraday screens', cause Faraday rotation of polarized emission from background sources, but do not depolarize. Any variation in strength or direction of the regular field within the volume traced by the telescope beam causes RM gradients and hence depolarization (Burn 1966; Sokoloff et al. 1998), which is similar to external Faraday dispersion (see below).

2.2 Faraday dispersion

Depolarization by IFD occurs in a region containing cosmic ray electrons, thermal electrons and turbulent magnetic fields and is given by

$$\mathrm{DP} = \frac{1-\mathrm{e}^{-S}}{S}, \tag{8}$$

where $S = 2\sigma_{RM}^2\lambda^4$. Depolarization by EFD in a non-emitting Faraday screen is given by

$$\mathrm{DP} = \mathrm{e}^{-S}. \tag{9}$$

The RM dispersion can be described in a simplified model of a turbulent magneto-ionic medium as

$$\begin{aligned}\sigma_{RM}^2 &= (0.81 n_e B_{turb} d)^2 f L/d \\ &\cong (0.81\langle n_e\rangle\langle B_{turb}\rangle)^2 L d/f,\end{aligned} \tag{10}$$

where n_e (in cm^{-3}) is the electron density within the turbulent cells of size d (the 'correlation length', in pc), L is the path-length (in pc), $\langle n_e\rangle$ is the average electron density in the volume along the path-length traced by the telescope beam, f is the filling factor of the cells ($f = \langle n_e\rangle/n_e$) and $\langle B_{turb}\rangle$ (in μG) is the mean strength of the turbulent magnetic field, assumed to be the same inside and outside of the cells. We further assume that the field direction is constant within each cell and that the contribution of the beamsize to σ_{RM} is negligible. If however the beamsize corresponds to a scale much larger than that of RM variations, σ_{RM} cannot be described by equation (10).

Note that other definitions of σ_{RM} in the literature used a different dependence on the filling factor f. Future high-resolution radio observations are needed which can directly measure σ_{RM}.

The effect of depolarization of the PI by internal and external Faraday dispersions is shown in Fig. 3 for $\alpha = 0.9$. The dependence of polarization intensity on wavelength is the same for both mechanisms at high frequencies where no depolarization occurs, while beyond the peak (at low frequencies) the PI decreases faster in the case of external Faraday dispersion. At low frequencies (before the maximum) the slopes of internal and external Faraday dispersion curves are significantly different: the spectrum is a power law ($P_\nu \propto \nu^{4-\alpha}$) for internal Faraday dispersion, while for external Faraday dispersion it deviates from a power law. The slope of the latter is estimated to be $\alpha \simeq 15$ between 1/10 and 1/100 of the maximum PI. The intensity fixed at the level of σ_{RM} reaches the peak at a slightly larger frequency for external Faraday dispersion than in the case of internal Faraday dispersion (Fig. 3).

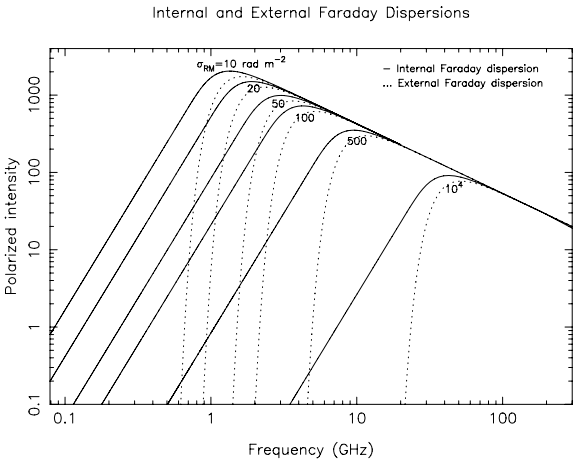

Figure 3. Polarized intensity for a spectral index of total synchrotron intensity of $\alpha = 0.9$ and depolarization by internal (solid line) and external (dashed line) Faraday dispersions at different levels of $\sigma_{\rm RM}$.

The equation for the optimum wavelength ($\lambda_{\rm opt}$) of maximum polarized emission in the case of internal RM dispersion is

$$e^{2S_o} - \frac{8S_o}{\alpha - 4} - 1 = 0, \quad (11)$$

where $S_o = 2\sigma_{\rm RM}^2\lambda_{\rm opt}^4$. For external RM dispersion we derive the equation

$$\lambda_{\rm opt} = \left(\frac{\alpha}{8\sigma_{\rm RM}^2}\right)^{1/4}, \quad (12)$$

where $\lambda_{\rm opt}$ is measured in m.

The dependence of the optimum frequency on internal dispersion (full line) and external (dotted line) dispersion is shown in Fig. 4 for $\alpha = 0.5, 0.9$ and 1.3. Polarized sources with larger $\sigma_{\rm RM}$ are best observed at high frequencies. In the case of internal RM dispersion, we found that $\lambda_{\rm opt} = A_1\sigma_{\rm RM}^{-0.5}$, where $A_1 = 0.6$, 0.7 and 0.87 for $\alpha = 0.5$, 0.9 and 1.3, respectively. For external RM dispersion the relations are $\lambda_{\rm opt} = A_2\sigma_{\rm RM}^{-0.5}$, where $A_2 = 0.50$, 0.58 and 0.63 for $\alpha = 0.5$, 0.9 and 1.3, respectively.

At long wavelength and/or large Faraday dispersion ($S \gg 1$), equation (9) can no longer be applied because the correlation length of polarized emission is smaller than the cell size d (Tribble 1991; Sokoloff et al. 1998), and the external depolarization by external dispersion becomes

$$\mathrm{DP} = (2\sigma_{\rm RM}\lambda^2)^{-1}. \quad (13)$$

This equation is valid only at wavelengths much longer than the optimum wavelength which corresponds to $S_o = \alpha/4 < 1$ (see equation 12) and hence is not relevant for this paper.

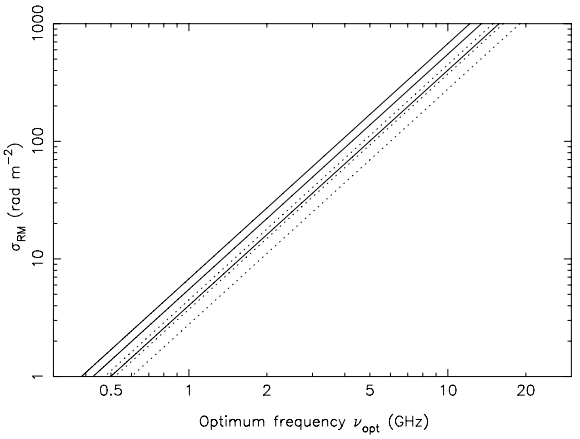

Figure 4. Optimum frequency of maximum polarized emission for a synchrotron spectrum with spectral index $\alpha = 0.5$, 0.9 and 1.3 (from bottom to top) and depolarized by internal (solid line) and external (dashed line) Faraday dispersions against RM dispersion.

2.3 Mixed cases

Many astrophysical media contain both regular and turbulent magnetic fields, while the descriptions of Faraday depolarization in Sections 2.1 and 2.2 are only valid if one type of magnetic fields dominates. In mixed cases with similar field strengths, the total depolarization can still be described by equation (8), where S becomes a complex number (Sokoloff et al. 1998). As an approximation, it may be assumed that some fraction of the emitting medium on the far side is totally depolarized by Faraday dispersion and the remaining volume on the near side is subject to depolarization by differential Faraday rotation. Here, the total depolarization is the product of equations (4) and (8) with appropriate weighting according to the strengths of the regular and turbulent field components.

2.4 RM grids

If RMs of a grid of bright, compact polarized sources behind extended foreground objects are measured, the foreground media act as Faraday screens and contribute to one single component in the Faraday spectrum. Only foreground regions with significant polarized emission may generate secondary peaks in the Faraday spectrum. The main depolarization mechanism for RM grids is EFR in the foreground (see Section 3). DFR and IFD may occur in the background sources, but are generally weak due to the small source sizes and are further reduced in distant objects by the RM dilution factor (see below).

3 DISCUSSION AND CONCLUSIONS

An observer planning polarization observations needs to investigate the expected range of |RM| and Faraday dispersion within a source. In Table 1 we compiled typical physical properties of magneto-ionic media in various astrophysical objects. The numbers may vary by a factor of several or are still uncertain, as in the case of the intracluster medium in galaxy clusters and of the intergalactic medium. The media are assumed to be 'simple', characterized by a single RM component and/or by an RM dispersion $\sigma_{\rm RM}$. The resulting optimum frequency bands give a first-order estimate for the range of highest polarized intensities.

Table 1 allows an observer to estimate which depolarization effect dominates in a medium: the larger the optimum frequency, the stronger is the depolarization. In discs and haloes of galaxies, DFR and IFD are of similar importance. In 'magnetic arms' between optical spiral arms, the regular field and hence DFR are strongest. In galaxy clusters, turbulent fields and hence IFD dominate.

The polarized emission of the inner discs, spiral arms, central regions of galaxies and the cores of galaxy clusters should be observed at wavelengths below a few centimetres (at frequencies beyond about 10 GHz), in order to avoid strong depolarization by DFR and IFD. Outer galaxy discs, galaxy haloes, haloes of galaxy clusters and intergalactic filaments have lower intrinsic |RM| and Faraday dispersion and are best observed at decimetre wavelengths (at frequencies below about 2 GHz). Polarized intensity from intergalactic filaments is low because the predicted magnetic fields

Table 1. Typical properties of diffuse magneto-ionic media and the corresponding optimum frequencies for polarization observations, assuming a synchrotron spectral index $\alpha = 0.9$.

Source	$\langle n_e \rangle$ (cm^{-3})	B_{reg} (μG)	B_{turb} (μG)	L (pc)	d (pc)	f	Reference	$\|RM\|^a$ (rad m^{-2})	$\nu_{opt}{}^b$ (GHz)	$\sigma_{RM}{}^a$ (rad m^{-2})	$\nu_{opt}{}^c$ (GHz)
Emitting and Faraday-rotating media											
Faint galaxy disc	0.01	5	5	1000	50	0.2	1	40	2.5	20	2.3
Bright galaxy disc	0.05	5	10	1000	50	0.5	2, 3	200	6	130	6
Spiral arm	0.1	2	20	500	50	0.5	3	80	3.8	360	10
Magnetic arm	0.03	10	5	500	50	0.5	2	120	4.3	27	2.7
Star-forming complex	0.5	<2	20	100	10	0.05	3	<80	<3.8	1100	15
Faint galaxy halo	0.01	1	3	1000	50	0.5	4	8	1.2	8	1.5
Bright galaxy halo	0.02	3	5	1000	50	0.5	4, 5	50	2.7	25	2.5
Galaxy cluster halo	0.001	<1	1–5	10^5	$(1–5) \times 10^4$	1?	6, 7	<80	<3.8	25–300	2.5–10
Galaxy cluster core	0.01	<1	10–30	10^4	3000	1?	8	<80	<3.8	500–1500	10–30
Galaxy cluster relic	10^{-4}	<1	1–5	$10^{6\,d}$	1000	1?	9	$<80^d$	<3.8	3–15	0.9–2
IGM filament	5×10^{-6}	<0.1	<0.3	$5 \times 10^{6\,d}$	5×10^5	1?	10	$<2^d$	$<0.6^e$	<2	$<0.75^e$
Faraday-rotating, non-emitting media ('Faraday screens')											
Local Milky Way[f]	0.03	2	3	200	50	0.5	11	10	1.3	10	1.7
Local Milky Way[g]	0.05	2	5	3000	50	0.5	11	80	3.8	80	5
IGM around radio lobes	0.001	<1	1–5	10^5	$(5–20) \times 10^3$	1?	12, 13	<80	<3.8	20–200	2.3–7.5

[a]Predicted; consistent with observations where available.
[b]Optimum frequency in case of differential Faraday rotation.
[c]Optimum frequency in case of internal Faraday dispersion.
[d]Projection dependent.
[e]Limited by the polarized emission of the Galactic foreground.
[f]High Galactic latitude.
[g]Low Galactic latitude.
References: (1) Fletcher et al. (2004); (2) Beck (2007); (3) Fletcher et al. (2011); (4) Hummel, Beck & Dahlem (1991); (5) Heesen et al. (2009); (6) Kim et al. (1990); (7) Murgia et al. (2004); (8) Vogt & Enßlin (2005); (9) van Weeren et al. (2010); (10) Xu et al. (2006); (11) Sun & Reich (2009); (12) Laing et al. (2008); (13) Feain et al. (2009).

are weak, but, due to the synchrotron spectrum, increases towards the metre-wave range where Faraday depolarization is still small. Observations with low-frequency telescopes such as LOFAR are promising, but difficult due to the strong Galactic foreground.

The observed Faraday dispersion in the nearby interstellar medium (ISM) of the Milky Way is about 10 rad m^{-2} at high latitudes and beyond 50 rad m^{-2} at low latitudes (Schnitzeler 2010), in agreement with the model of Sun & Reich (2009). EFD in the Galactic foreground with an RM dispersion of 60–160 rad m^{-2} at low Galactic latitudes (Sun & Reich 2009) yields an optimum observation wavelength of 5–7 cm, while about 20 cm (1.5 GHz) at high Galactic latitudes. The all-sky RM surveys with the SKA (Gaensler, Beck & Feretti 2004) and its pathfinder ASKAP [project Polarisation Sky Survey of the Universe's Magnetism (POSSUM); Gaensler, Landecker & Taylor 2010] and deep RM grids towards nearby galaxies and galaxy clusters with the MeerKAT and APERTIF telescopes are planned around 1 GHz. At the low frequencies observed with LOFAR, the polarized emission of the Galactic foreground is affected by Faraday rotation and strongly fluctuates with position and frequency, which hampers the detection of signals from extragalactic objects.

Sources with extremely large intrinsic RM ($|RM| \gtrsim 10^4$ rad m^{-2}) or large RM dispersion ($\sigma_{RM} \gtrsim 10^4$ rad m^{-2}) are rare. Extreme rotation measures are measured for core-dominated quasars, e.g. 3C 273 ($\approx +4 \times 10^4$ rad m^{-2} over the range 43–86 GHz; Attridge et al. 2005), and for the Galactic Centre, Sgr A* ($\approx -5 \times 10^5$ rad m^{-2} over the range 150–400 GHz; Macquart et al. 2006; Marrone et al. 2007). Sources with such large intrinsic RM will escape detection in polarization with the upcoming radio surveys (e.g. POSSUM) because of strong depolarization around 1.4 GHz (see Figs 1 and 3). The optimum frequency band of such objects is beyond about 30 GHz and they can be targeted by mm-wave telescopes operating at sufficiently high frequencies [e.g. Atacama Large Millimeter Array (ALMA)]. The innermost regions of jets of core-dominated quasars, cores of massive galaxy clusters and starburst galaxies having dense turbulent gas and strong magnetic fields are candidates for such extreme values of RM or σ_{RM}.

The optimum wavelength band to observe distant polarized sources is larger than that for nearby ones. The intrinsic |RM| and intrinsic RM dispersion of distant objects observed at a fixed frequency are smaller by a factor of $(1 + z)^{-2}$ and, hence, Faraday depolarization is smaller and the degree of polarization is higher (Fig. 1). The optimum wavelength band to observe a nearby bright galaxy disc with $|RM|(z = 0) = 200$ rad m^{-2} is around 5 cm (6 GHz; see Table 1). If we want to observe the same source, for example at $z = 3$, then the observed $|RM|(z = 3) \simeq 12$ rad m^{-2} and the optimum wavelength band for observation is around 20 cm (1.4 GHz). The optimum wavelength band to observe a cluster core with $\sigma_{RM}(z = 0) \simeq 1000$ rad m^{-2} (Table 1) at $z = 3$ is around 7 cm (4 GHz). Hence, cluster cores and bright disc galaxies at high redshifts can be detected with ASKAP and the high-frequency SKA array.

Most of the distant sources detected with future sensitive radio telescopes will be from the population of star-forming galaxies

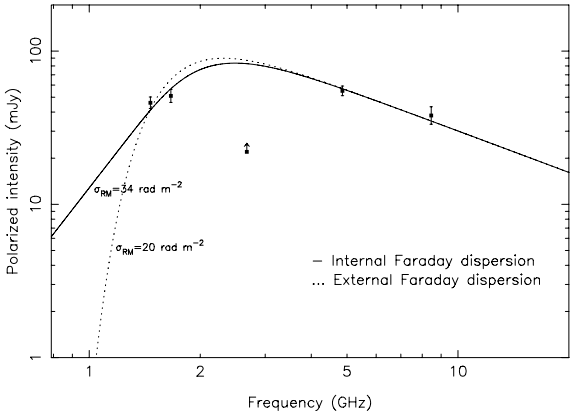

Figure 5. Spectrum of integrated polarized flux densities of the spiral galaxy NGC 6946 and fits with IFD and EFD. The data are computed from the maps by Beck (2007) with the same resolution of 15 arcsec, except for the map centred at 2.675 GHz with 4.4-arcmin resolution which yields a lower limit.

which can be expected to be more polarized at larger distance where depolarization is smaller. On the other hand, the detection of regular magnetic fields via RM from intervening galaxies on the line of sight towards polarized background sources (Bernet et al. 2008; Kronberg et al. 2008) will become more difficult for distant galaxies because their |RM| is lower.

Depolarization in galaxies can be well described by Faraday dispersion. An example for the spiral galaxy NGC 6946 is shown in Fig. 5. The spectrum of integrated polarized flux densities is fitted by an IFD model (equation 8) with $\sigma_{\rm RM} \simeq 34$ rad m^{-2}, in excellent agreement with the analysis of the depolarization map by Beck (2007), or by an EFD model (equation 9) with $\sigma_{\rm RM} \simeq 20$ rad m^{-2} from the Galactic foreground. With only one more observation at a frequency band below 1.4 GHz, IFD and EFD can be distinguished. Note that such integrated data cannot be fitted by a DFR model because the variation in RM across the galaxy smooths out the sharp minima seen in Fig. 1. DFR can only be detected in objects with constant RM.

In this paper we demonstrated that measurement of the spectrum of PI around the optimum frequency offers a simple first-order method to measure the average |RM| or the average Faraday dispersion in media with a simple structure or strong turbulence, without knowledge of polarization angles. Moreover, the knowledge of the optimum frequency and hence the main (first) maximum of the PI spectrum is important for performing RM synthesis. It is presumed that a range around the optimum frequency is included in the observed spectral range to ensure the recovery of the main peak of the RM transfer function which is needed to clean the Faraday spectrum (Heald 2009). Sufficiently wide coverage in frequency is also needed to distinguish between varieties of depolarization effects.

We also showed that the slope of the PI spectrum at low frequencies is much steeper for EFD than for IFD (Fig. 4). This allows us to distinguish between these two effects, which is hardly possible with other methods. DFR has a similarly steep spectrum as EFD, but is easily recognizable by its periodic fluctuations, leading to total depolarization at certain wavelengths (Fig. 1).

If the synchrotron-emitting and Faraday-rotating medium has a complicated structure but is not strongly turbulent, a spectrum of components in Faraday space is expected, no well-defined peak of the PI spectrum can be found and the results of this paper cannot be applied. A model for two Faraday depth components was discussed by Farnsworth, Rudnick & Brown (2011). Two-component Faraday spectra have been detected e.g. towards the inner regions of a few spiral galaxies (Heald, Braun & Edmonds 2009), possibly due to a different field configuration in the nuclear region or a reversal of the radial field components on the near and far sides of the nucleus. Faraday spectra towards radio galaxies located in the inner parts of galaxy clusters also reveal multiple components which may emerge from the lobes (Pizzo et al. 2011). The fraction of multicomponent Faraday spectra of ISM regions in the Milky Way is still unclear. While most spectra towards the Perseus cluster near the Galactic plane are complicated (Brentjens 2011), the ISM near the Galactic anticentre is Faraday-quiet (Schnitzeler et al. 2009). The forthcoming all-sky RM survey Global Magneto-Ionic Medium Survey (GMIMS; Landecker 2010) will bring us more clarity.

ACKNOWLEDGMENTS

This work was supported by the European Community Framework Programme 6, Square Kilometre Array Design Study (SKADS). TGA acknowledges support by DFG–SPP project under grant 566960. We thank Luigina Feretti and Torsten Enßlin for help in compiling cluster data for Table 1, as well as Roberto Pizzo, Wolfgang Reich, Dominic Schnitzeler, Rodion Stepanov and Dmitry Sokoloff for useful discussions.

REFERENCES

Attridge J. M., Wardle J. F. C., Homan D. C., 2005, ApJ, 633, L85
Beck R., 2007, A&A, 470, 539
Beck R., Brandenburg A., Moss D., Shukurov A., Sokoloff D., 1996, ARA&A, 34, 155
Bernet M. L., Miniati F., Lilly S. J., Kronberg P. P., Dessauges-Zavadsky M., 2008, Nat, 454, 302
Brentjens M. A., 2011, A&A, 526, A9
Brentjens M. A., de Bruyn A. G., 2005, A&A, 441, 1217
Burn B. J., 1966, MNRAS, 133, 67
Conway R. G., Haves P., Kronberg P. P., Stannard D., Vallee J. P., Wardle J. F. C., 1974, MNRAS, 168, 137
Farnsworth D., Rudnick L., Brown S., 2011, AJ, 141, 191
Feain I. J. et al., 2009, ApJ, 707, 114
Fletcher A., Shukurov A., 2006, MNRAS, 371, L21
Fletcher A., Berkhuijsen E. M., Beck R., Shukurov A., 2004, A&A, 414, 53
Fletcher A., Beck R., Shukurov A., Berkhuijsen E. M., Horellou C., 2011, MNRAS, 412, 2396
Frick P., Sokoloff D., Stepanov R., Beck R., 2010, MNRAS, 401, L24
Frick P., Sokoloff D., Stepanov R., Beck R., 2011, MNRAS, 414, 2540
Gaensler B. M., Beck R., Feretti L., 2004, New Astron. Rev., 48, 1003
Gaensler B. M., Landecker T. L., Taylor A. R., 2010, BAAS, 42, 470
Heald G., 2009, in Strassmeier K. G., Kosovicher A. G., Beckman J. E., eds, Cosmic Magnetic Fields: From Planets, to Stars and Galaxies. Cambridge Univ. Press, Cambridge, p. 591
Heald G., Braun R., Edmonds R., 2009, A&A, 503, 409
Heesen V., Krause M., Beck R., Dettmar R.-J., 2009, A&A, 506, 1123
Hummel E., Beck R., Dahlem M., 1991, A&A, 248, 23
Kim K.-T., Kronberg P. P., Dewdney P. E., Landecker T. L., 1990, ApJ, 355, 29
Kronberg P. P., Conway R. G., Gilbert J. A., 1972, MNRAS, 156, 275
Kronberg P. P., Bernet M. L., Miniati F., Lilly S. J., Short M. B., Higdon D. M., 2008, ApJ, 676, 70
Laing R. A., Bridle A. H., Parma P., Murgia M., 2008, MNRAS, 391, 521
Landecker T. L., 2010, in Kothes R., Landecker T. L., Willis A. G., eds, ASP Conf. Ser. Vol. 438, The Dynamic Interstellar Medium. Astron. Soc. Pac., San Francisco, p. 261

Macquart J.-P., Bower G. C., Wright M. C. H., Backer D. C., Falcke H., 2006, ApJ, 646, L111
Marrone D. P., Moran J. M., Zhao J.-H., Rao R., 2007, ApJ, 654, L57
Murgia M., Govoni F., Feretti L., Giovannini G., Dallacasa D., Fanti R., Taylor G. B., Dolag K., 2004, A&A, 424, 429
Pizzo R. F., de Bruyn A. G., Bernardi G., Brentjens M. A., 2011, A&A, 525, A104
Schnitzeler D. H. F. M., 2010, MNRAS, 409, L99
Schnitzeler D. H. F. M., Katgert P., de Bruyn A. G., 2009, A&A, 494, 611
Sokoloff D. D., Bykov A. A., Shukurov A., Berkhuijsen E. M., Beck R., Poezd A. D., 1998, MNRAS, 299, 189 (erratum in MNRAS, 303, 207)
Sun X. H., Reich W., 2009, A&A, 507, 1087
Sun X. H., Reich W., Han J. L., Reich P., Wielebinski R., Wang C., Müller P., 2011, A&A, 527, A74
Tabara H., Inoue M., 1980, A&AS, 39, 379
Tribble P. C., 1991, MNRAS, 250, 726
van Weeren R. J., Röttgering H. J. A., Brüggen M., Hoeft M., 2010, Sci, 330, 347
Vogt C., Enßlin T. A., 2005, A&A, 434, 67
Xu Y., Kronberg P. P., Habib S., Dufton Q. W., 2006, ApJ, 637, 19

This paper has been typeset from a TEX/LATEX file prepared by the author.